



Contents lists available at ScienceDirect

Bioorganic & Medicinal Chemistry Letters

journal homepage: www.elsevier.com/locate/bmcl

The discovery of reverse tricyclic pyridone JAK2 inhibitors. Part 2: Lead optimization



Tony Siu^{a,*}, Sathyajith E. Kumarasinghe^a, Michael D. Altman^b, Matthew Katcher^a, Alan Northrup^a, Catherine White^a, Craig Rosenstein^c, Anjili Mathur^d, Lin Xu^e, Grace Chan^c, Eric Bachman^d, Melaney Bouthillette^f, Christopher J. Dinsmore^a, C. Gary Marshall^g, Jonathan R. Young^a

^a Department of Medicinal Chemistry, Merck & Co., 33 Avenue Louis Pasteur, Boston, MA 02115, USA

^b Department of Structural Chemistry, Merck & Co., 33 Avenue Louis Pasteur, Boston, MA 02115, USA

^c Department of In Vitro Sciences, Merck & Co., 33 Avenue Louis Pasteur, Boston, MA 02115, USA

^d Department of Pharmacology, Merck & Co., 33 Avenue Louis Pasteur, Boston, MA 02115, USA

^e Department of Drug Metabolism, Merck & Co., 33 Avenue Louis Pasteur, Boston, MA 02115, USA

^f Department of Basic Pharmaceutical Sciences, Merck & Co., 33 Avenue Louis Pasteur, Boston, MA 02115, USA

^g Department of Oncology, Merck & Co., 33 Avenue Louis Pasteur, Boston, MA 02115, USA

ARTICLE INFO

Article history:

Received 7 January 2014

Revised 31 January 2014

Accepted 4 February 2014

Available online 15 February 2014

Keywords:

JAK2

Kinases

Water interaction

Kinase selectivity

Ligand binding affinity

Kinase partition index

Molecular modeling

ABSTRACT

This communication discusses the discovery of novel reverse tricyclic pyridones as inhibitors of Janus kinase 2 (JAK2). By using a kinase cross screening approach coupled with molecular modeling, a unique inhibitor–water interaction was discovered to impart excellent broad kinase selectivity. Improvements in intrinsic potency were achieved by utilizing a rapid library approach, while targeted structural changes to lower lipophilicity led to improved rat pharmacokinetics. This multi-pronged approach led to the identification of **31**, which demonstrated encouraging rat pharmacokinetics, in vivo potency, and excellent off-target kinase selectivity.

© 2014 Elsevier Ltd. All rights reserved.

The Janus kinases, (JAK1, JAK2, JAK3, and TYK2), are a family of non-receptor tyrosine kinases that mediate cytokine signaling and play a central role in regulating cell proliferation and immune response.¹ Most notably, JAK2 has attracted significant attention due to the discovery of the JAK2 V617F gain of function mutation and its causative link to polycythemia vera (PV), essential thrombocythemia (ET), and primary myelofibrosis (MF).² These findings prompted the initiation of numerous JAK2 medicinal chemistry programs,³ leading to over 60 clinical investigations of JAK2 inhibitors and ultimately resulting in the approval of Ruxolitinib for MF.⁴

In a previous communication, we reported the discovery and optimization of a novel JAK2 tricyclic pyridone inhibitor **1** (Fig. 1) from a screening hit to a lead compound suitable for in vivo proof of concept.⁵ Our initial strategy focused on monitoring ligand binding efficiency (LBE) while relying on structural information in con-

junction with a rapid library approach to afford **1**, which has excellent LBE (0.49), intrinsic potency (enzyme JAK2 IC₅₀ = 1 nM),⁶ cell potency (cell JAK2 IC₅₀ = 40 nM),⁷ and demonstrated in vivo PK/PD activity (IC₅₀ = 2700 nM).⁸ Despite the excellent in vitro and modest in vivo JAK2 potency, **1** and analogs within this series of fused naphthyridinones suffered from notable liabilities that required optimization before advancing further in development. In order to minimize unforeseeable adverse effects and toxicity due to broad inhibition of cellular processes, a stringent selectivity window of 100 fold or greater against a broad spectrum of kinases was required. Furthermore, despite the excellent in vitro potency of **1**, the in vivo properties of **1** required additional optimization to achieve more efficient dosing. In this communication, we expand upon our initial SAR findings and detail the optimization of kinase selectivity and in vivo properties leading to the identification of **31**.

Compound **1**, although quite potent against JAK2, is also a potent inhibitor of a variety of kinases as tested against a broad 98 kinase panel (89% of kinases >100 fold over JAK2⁹ with a partition

* Corresponding author. Tel.: +1 617 939 0216.

E-mail address: tony_siu@merck.com (T. Siu).

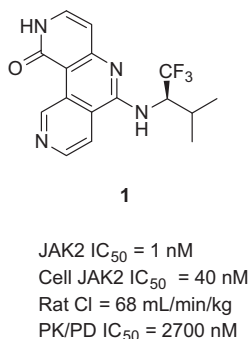


Figure 1. Lead identification hit for JAK2.

index¹⁰ of 0.56) (Fig. 3). Moreover, the kinase profiles of various other related analogs did not offer improvements in kinase selectivity, which is consistent with the modeled binding mode for this class of inhibitors. As discussed in a previous communication,⁵ our strategy for introducing chemical diversity was to utilize a varied set of amines to fill the ribose pocket space (Fig. 2). However, further diversification in this vector would presumably not significantly alter the kinase selectivity to the desired levels due to the high conservation of residues among kinases in this pocket. Furthermore, we imagined that branching out of the enzyme into the solvent front would also not improve selectivity since the inhibitor would not make contact with the enzyme surface.

In order to cross-fertilize kinase programs and to leverage serendipity, Merck Research Laboratories implemented a cross-screening effort between JAK2 and other Merck kinase programs. This cross-program collaboration led to the identification of **3**, where by the amino pyridine **2** was altered to its regio isomer (Scheme 1).

While this subtle core modification did not affect intrinsic potency, significant improvements in selectivity against a mini panel of off-target kinases were observed. Based on this serendipitous discovery, we were motivated to further expand upon this initial finding. Because the chemistry lent itself to a divergent synthesis, a library approach was utilized to rapidly generate diverse SAR.

The synthesis of the fused naphthyridinone core of **3** was performed in an analogous manner to **1** (Scheme 2).¹¹ Starting with 2-ethoxy nicotinic acid **4**, chlorination with oxalyl chloride followed by the addition of diisopropyl amine afforded amide **5**. With the diisopropyl amide in place, directed *ortho* lithiation with *sec*-BuLi followed by trapping of the anion with trimethylborate furnished boronic acid **6**. Suzuki cross coupling of boronic acid **6** with commercially available amino pyridine **7**, catalyzed by tetrakis palladium (0) triphenylphosphine, provided the coupled biaryl product **8**. Base induced ring closure with sodium bis(trimethylsilyl)amide (NaHMDS) afforded **9** as a poorly soluble polyaromatic molecule. Compound **9** was then subsequently heated in neat phosphoryl chloride at 100 °C in a microwave reactor resulting in a mixture of double chlo-

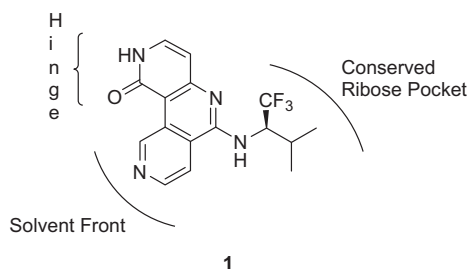
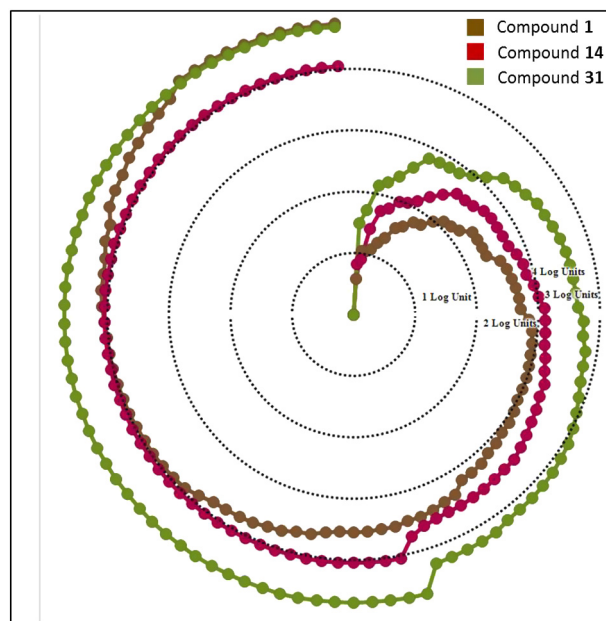
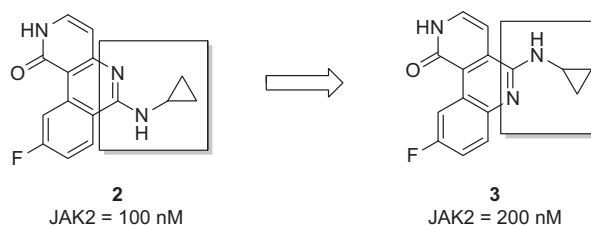


Figure 2. General binding of fused naphthyridones to JAK2 kinase.



Compounds	% Kinases >100X over JAK2	Partition Index ¹⁰
1	89	0.56
14	94	0.70
31	98	0.92

Figure 3. Kinase selectivity comparison of compounds **1**, **14**, and **31** against 98 kinases using a radar plot, percent of kinases >100 fold over JAK2, and partition index.¹⁰

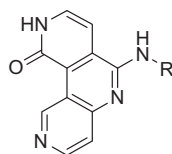


Scheme 1. Reversal of amino pyridine leads to increased kinase selectivity.

mination **10b** and monochlorination **10a** intermediates. Late stage intermediates **10a** and **10b** allowed for rapid analog generation, and thus a set of amines were substituted thermally at 65 °C with base assistance using sodium *tert*-butoxide. Final deprotection of the ethoxy ether **11a** with boron tribromide or acid hydrolysis of the chloro **11b** with 6 N HCl, yielded the pyridone analogs.

Table 1 summarizes the potency of a select set of amine and anilines. The focus of this library was to improve on the intrinsic JAK2 potency of **3** through enhanced contact with the enzyme and to evaluate the overall kinase selectivity for this new class of compounds. Initially, trifluoroamine **13** was prepared based on the favorable activity of **1**. Although **13** was active in enzyme and cells, the shift in potency with respect to **1** indicated that the SAR generated in our previous communication did not directly translate to the reverse pyridine series. Gratifyingly, 2,6-disubstituted anilines were quickly discovered to possess exquisite enzyme and cellular potency, highlighted by a focused library (**14–20**). The increased potency of the *ortho* aniline substituents of these compounds underscored the importance of a conformationally twisted aniline

Table 1
SAR of fused naphthyridinone analogs



Compound	R	JAK2 IC ₅₀ (nM)	Cell JAK2 IC ₅₀ (nM)
13		10	170
14		0.9	15
15		7	90
16		0.8	14
17		2	24
18		3	140
19		1	49
20		9	90

ring to enhance hydrophobic interactions in the ribose pocket and glycine rich loop. In an optimized case, 2,4,6-tri-halogenes were preferred as exemplified by **14** (JAK2 IC₅₀ = 0.9 nM and cell JAK2 IC₅₀ = 15 nM).

Having optimized for potency, **14** was profiled in a broad kinase panel consisting of 98 kinases and compared to **1** as shown in Figure 3.⁹ Kinase selectivity is depicted using a radar plot where the distance from the center is proportional to the fold selectivity over JAK2 in log₁₀ units. From the depiction of data in Figure 3, it can be observed that **14** is more selective because its curve lies outside that of **1**. Further metrics to highlight the improved selectivity were the increased number of kinases greater than 100-fold over JAK2 (94%) as well as an improved partition index¹⁰ (0.70) as compared to **1**.

In order to better understand the nature of the improved kinase selectivity, inhibitors **1** and **14** were modeled into a JAK2 crystal structure (Fig. 4).¹² As previously discussed, the pyridone of **1** is proposed to hydrogen bond to hinge residues Glu-930 and Leu-932. Furthermore, the CF₃ amine linkage may occupy the ribose

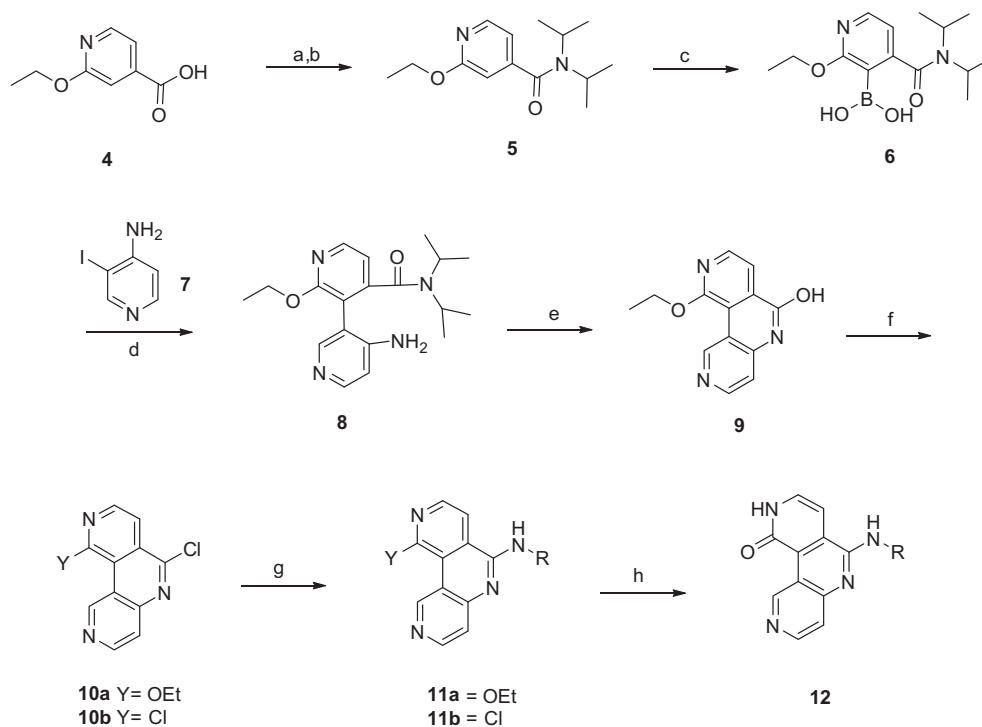
pocket of the enzyme with the NH pointing towards the solvent front.⁵ Compound **14** is proposed to bind to the hinge in a manner similar to **1**, with the aniline functional group making favorable hydrophobic interactions in the ribose pocket and with the NH of the aniline pointing towards the back pocket. Modeling suggests that the reversed amino pyridine of **14** allows the NH to interact with a bound water molecule (H₂O-139 in PDB 2B7A) which in turn forms hydrogen bonds with the backbone of residues Gly-993 and Asp-994. The presence of this crystallographic water molecule may be a consequence of the unique conformation of Gly-993 where the backbone is flipped relative to the DFG-1 residues of most other kinases.¹³ This unique interaction possibly helps to generate more specific affinity towards the JAK2 enzyme in particular enzyme in particular.¹⁴

In pharmacokinetic studies, **14** showed a moderate rat plasma clearance (41 mL/min/kg) and volume (2.6 L/kg) and a short half-life (0.8 h). Moreover, **14** was profiled in our in vivo PK/PD model, where it displayed an IC₅₀ of 2300 nM. Thus, despite advances in the in vitro properties and the improved kinase selectivity of **14** as compared to **1**, the modest rat CI and in vivo potency highlighted the need for further optimization.

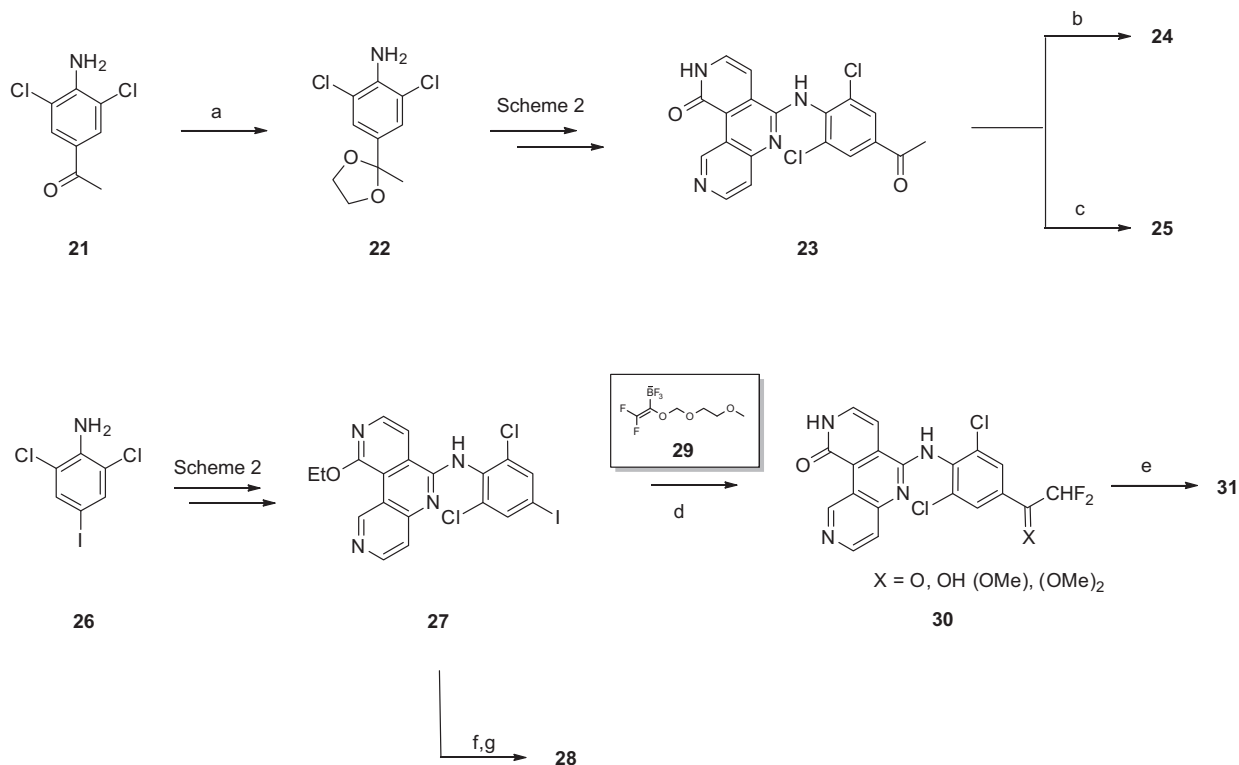
To address the pharmacokinetics and in vivo potency, we focused on improving the physicochemical properties by lowering the lipophilicity, and hence the log*D* of **14**. The reduction of intrinsic lipophilicity is central to our strategy to increase the stability of our compounds towards oxidative metabolism.¹⁵ The computational docking model of **14** (Fig. 4) suggested that the aromatic 4-fluorine of the aniline might be amendable to structural changes since it occupies an open pocket and does not come in contact with specific interactions with the enzyme backbone. Modifications were aimed at introducing polar functional groups to influence physicochemical properties. Additionally, we noticed an opportunity to possibly interact with the carbonyl of Asn-981, and hence our designs for modifying log*D* in this area focused on heteroatoms with hydrogen bond donating capabilities (Fig. 5).

To access this series of compounds with modifications at the aniline 4-position, further synthetic transformations were needed (Scheme 3).¹¹ Starting with 1-(4-amino-3,5-dichlorophenyl)ethanone **21**, ketal formation under acidic conditions afforded the ketal **22**. Masking the ketone was necessary in order to disrupt nitrogen lone pair conjugation to the ketone and increase the nucleophilicity of the aniline for addition to the tricyclic core. This protected aniline was carried through to **23** using the same conditions as in Scheme 2, followed by deprotection with boron tribromide. Sodium borohydride reduction of the ketone provided secondary alcohol **24**.¹⁶ Alternatively, treatment of the ketone with excess methyl magnesium bromide afforded the tertiary alcohol **25**. Additional methods to functionalize the *para* position of the aniline utilized palladium cross coupling chemistry. 2,6-Dichloro-4-iodoaniline was introduced into tricyclic core **10a** according to the methods described in Scheme 2. Suzuki reaction of **27** with pyrazole-5-ylboronic acid followed by deprotection with boron tribromide yielded **28**. Additionally, **27** could be deprotected and cross coupled with boron trifluoride salt **29**¹⁷ to afford **30** as a mixture of ketone and ketals. This mixture was treated with sodium borohydride to afford hydride to afford **31**.¹⁶

With ready access to substituted anilines in hand, we tested our hypothesis of improving in vivo properties through manipulation of the overall physicochemical property of the molecule (Table 2). Analogs identified which maintained high JAK2 cell potency were profiled in rat PK studies, followed by evaluation in our in vivo PK/PD model.¹⁸ In order to compare PK properties among compounds, we accounted for the differences in plasma protein binding by normalizing the rat total CI to the rat unbound CI, a key parameter to assess improvements in PK. As an initial exploration to decrease the log*D*, we tested sulfonamide **32**. The introduction

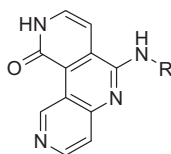


Scheme 2. Synthesis of fused naphthyridinones. Reagents and conditions: (a) oxalyl chloride, CH_2Cl_2 ; (b) diisopropyl amine, triethylamine, CH_2Cl_2 ; (c) *sec*-BuLi, trimethylborate, -78°C , THF; (d) 7, $\text{Pd}(\text{PPh}_3)_4$, 2.0 M Na_2CO_3 , 100°C , THF; (e) NaHMDS, 0°C , THF; (f) POCl_3 , 100°C , microwave; (g) sodium *tert*-butoxide, amines, 85°C , THF; (h) Y = OEt, BBr_3 , 85°C , CHCl_3 or Y = Cl, 6 N HCl dioxane, 85°C .



Scheme 3. Synthesis of fused naphthyridinones with substituted anilines. Reagents and conditions: (a) ethylene glycol, PPTs, 100°C , benzene; (b) NaBH_4 , MeOH; (c) (5 equiv) 1.0 M MeMgBr in THF/toluene, 0°C , THF; (d) (i) Et_3N , $\text{PdCl}_2(\text{dppf})\text{-CH}_2\text{Cl}_2$, 29, 90°C , *n*-PrOH; (ii) BBr_3 , 85°C , CHCl_3 ; (e) NaBH_4 , MeOH; (f) $\text{Pd}(\text{PPh}_3)_4$, 2.0 M NaHCO_3 , 1H-pyrazole-5-boronic acid, 80°C , THF; (g) BBr_3 , 85°C , CH_2Cl_2 .

Table 2
SAR of 4-substituted anilines



R	JAK2 enzyme/cell IC ₅₀ (nM)	HplcLogD	Rat PPB % bound	Rat Cl (mL/min/kg)	Unbound rat Cl (mL/min/kg)	PK/PD IC ₅₀ (nM)
	0.9/15	1.75	95.2	42	875	2300
	0.6/12	1.20	95.2	54	1125	400
	0.5/18	1.34	97.4	29	1115	1200
	1/37	1.43	99.9	10	10,000	NA
	0.2/26	1.46	97.2	16	571	1300
	0.15/113	1.17	NA	50	NA	NA

of a sulfonamide moiety lowered the logD by half a log unit as compared to **14** and increased the overall JAK2 affinity (IC₅₀ = 0.15 nM). This result further validated our hypothesis that additional polarity could be introduced in this flexible region of the kinase. However, the increased polarity dramatically affected the cell shift by >700 fold. Further investigation with 2-pyrazole **28** resulted in lower logD while maintaining favorably potency; however, this functional group offered no PK advantage (unbound Cl = 10000 mL/min/kg) with respect to **14**. Polar groups such as alcohols were also investigated as attractive groups to lower lipophilicity. To that end, alcohol **24** was profiled and showed poor rat PK (unbound Cl = 1125 mL/min/kg), but with a much improved in vivo potency (PK/PD IC₅₀ = 400 nM). Despite the poor rat unbound Cl, we were encouraged with the potency and favorable logD associated with the alcohol functional group. We hypothesized that the rapid metabolism of **24** could occur through the glucuronidation or oxidation of the alcohol functionality, and that blocking or attenuating these events would be beneficial for improving the rat pharmacokinetic properties. Consequently, both **25** and **31** were synthesized with the goal of attenuating the trans-

formation of the alcohol with steric and electronic features. Disappointingly, tertiary alcohol **25** still suffered from high rat unbound Cl (1115 mL/min/kg); however, difluoro methyl alcohol **31** had an improved rat unbound Cl (571 mL/min/kg), validating our hypothesis. Furthermore, **31** was tested in our PK/PD assay and displayed a respectable in vivo potency of 1300 nM. Although modest potency gains were made in vivo, when combined with the improved rat unbound Cl, **31** possessed a more desirable in vivo profile than **14**. Along with the improved in vivo properties, the addition of the OH to Asn-981 interaction contributed to further increasing the kinase selectivity of **31** with notable improvements compared to **1** in the radar plot, 100-fold JAK2 selectivity over 98% of the kinase panel, and a partition index¹⁰ of 0.92.

In this communication, we detailed the strategy and approach used to optimize our initial JAK2 leads into inhibitors with favorable drug like properties. By using a kinase cross-screening approach to leverage our internal network capabilities, we discovered the reversed pyridine **3** as a critical SAR to improve kinase selectivity. While a rapid library approach aided in identifying analogs which improved intrinsic potency by 200-fold, molecular

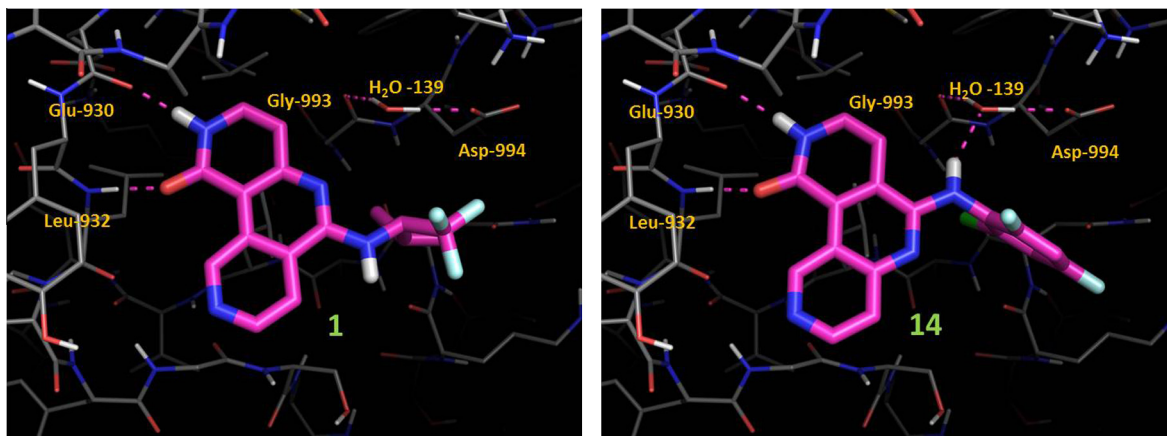


Figure 4. Inhibitors **1** and **14** modeled in a JAK2 crystal structure showing the unique interaction of **14** with water-139.

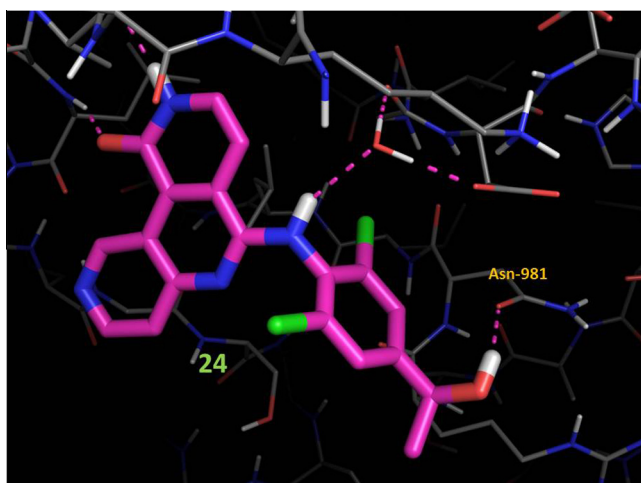


Figure 5. Inhibitor **24** modeled in ATP binding site of JAK2 enzyme highlighting potential interaction with Asn-981.

modeling studies provided valuable insights into the improved kinase selectivity. These results, together with monitoring physico-chemical properties and lipophilicity, led to the discovery of **31**, a kinase selective JAK2 inhibitor with favorable in vivo properties.

Acknowledgments

T.S. thanks Kerrie Spencer, Meredith McGowan, Jongwon Lim, and Andrew Haidle for careful reading of this manuscript and Bruce Adams for NMR support.

References and notes

- Vainchenker, W.; Constantinescu, S. N. *Oncogene* **2013**, *32*, 2601.
- Reddy, M. M.; Deshpande, A.; Sattler, M. *Expert Opin. Ther. Targets* **2012**, *16*, 313.
- (a) Antonyamsy, S.; Hirst, G.; Park, F.; Sprengler, P.; Stappenbeck, F.; Steensma, R.; Wilson, M.; Wong, M. *Bioorg. Med. Chem. Lett.* **2009**, *19*, 279; (b) Burns, C. J.; Bourke, D. G.; Andrau, L.; Bu, X.; Charman, S. A.; Donohue, A. C.; Fantino, E.; Farrugia, M.; Feutrill, J. T.; Joffe, M.; Kling, M. R.; Kurek, M.; Nero, T. L.; Nguyen, T.; Palmer, J. T.; Phillips, I.; Shackelford, D. M.; Sikanyika, H.; Styles, M.; Su, S.; Treutlein, H.; Zeng, J.; Wilks, A. F. *Bioorg. Med. Chem. Lett.* **2009**, *19*, 5887; (c) Ioannidis, S.; Lamb, M. L.; Wang, T.; Almeida, L.; Block, M. H.; Davies, A. M.; Peng, B.; Su, M.; Zhang, H.-J.; Hoffmann, E.; Rivard, C.; Green, I.; Howard, T.; Pollard, H.; Read, J.; Alimzhanov, M.; Bebernitz, G.; Bell, K.; Ye, M.; Huszar, D.; Zinda, M. *J. Med. Chem.* **2011**, *54*, 262; (d) Lim, J.; Taoka, B.; Otte, R. D.; Spencer, K.; Dinsmore, C. J.; Altman, M. D.; Chan, G.; Rosenstein, C.; Sharma, S.; Su, H.-P.; Szewczak, A. A.; Xu, L.; Yin, H.; Zugay-Murphy, J.; Marshall, C. G.; Young, J. R. *J. Med. Chem.* **2011**, *54*, 7334; (e) Harikrishnan, L. S.; Kamau, M. G.; Wan, H.; Inghrim, J. A.; Zimmermann, K.; Sang, X.; Mastalerz, H. A.; Johnson, W. L.; Zhang, G.; Lombardo, L. J.; Poss, M. A.; Trainor, G. L.; Tokarski, J. S.; Lorenzi, M. V.; You, D.; Gottardis, M. M.; Bladwin, K. F.; Lippy, J.; Nirschi, D. S.; Qui, R.; Miller, A. V.; Khan, J.; Sack, J. S.; Purandare, A. V. *Bioorg. Med. Chem. Lett.* **2011**, *21*, 1425; (f) Labadie, S.; Barrett, K.; Blair, W. S.; Chang, C.; Deskmukh, G.; Eigenbrot, C.; Gibbons, P.; Johnson, A.; Kenny, J. R.; Kohli, P. B.; Liimatta, M.; Lupardus, P. J.; Shia, S.; Steffek, M.; Ubhayakar, S.; van Abbema, A.; Zak, M. *Bioorg. Med. Chem. Lett.* **2013**, *21*, 5923.
- Harry, B. L.; Eckhardt, S. G.; Jimeno, A. *Expert Opin. Ther. Targets* **2012**, *21*, 637.
- Siu, T.; Kozina, E. S.; Jung, J.; Rosenstein, C.; Mathur, A.; Altman, M. D.; Chan, G.; Xu, L.; Bachman, E.; Mo, J.; Bouthillette, M.; Rush, T.; Dinsmore, C. J.; Marshall, C. G.; Young, J. R. *Bioorg. Med. Chem. Lett.* **2010**, *20*, 7421.
- Detection of peptide phosphorylation was performed by homogenous time resolved fluorescence (HTRF) using a europium chelate. IC₅₀ values are reported as the averages of at least two independent determinations; standard deviations are within +/- 25–50% of IC₅₀ values. For further details see: WO2009035575.
- Detection of STAT phosphorylation was performed using AlphaScreen™ SureFire™ p-STAT5 assay (Perkin Elmer and TGR Biosciences) using both biotinylated anti-phospho-STAT5 antibody, which is captured by Streptavidin-coated Donor beads, and anti-total STAT5 antibody, which is captured by Protein A conjugated Acceptor beads. IC₅₀ values are reported as the averages of at least two independent determinations; standard deviations are within +/- 25–50% of IC₅₀ values. For further details see: WO2008156726.
- Mathur, A.; Mo, J.; Kraus, M.; O'Hare, E.; Sinclair, P.; Young, J.; Zhao, S.; Wang, Y.; Kopinja, J.; Qu, X.; Reilly, J.; Walker, D.; Xu, L.; Aleksandrowicz, D.; Marshall, C. G.; Scott, M. L.; Kohl, N. E.; Bachman, E. *Biochem. Pharmacol.* **2009**, *78*, 382.
- Compounds **1**, **14**, and **31** were tested against a broad panel of 98 kinases at Invitrogen. Selectivity folds were calculated based on estimated IC₅₀s from 3 point titrations (1, 100, 1000 nM) and the internal JAK2 potencies.
- Cheng, A. C.; Eksterowicz, J.; Geuns-Meyer, S.; Sun, Y. *J. Med. Chem.* **2010**, *53*, 4502.
- For full experimental procedure see WO2009035575.
- Compounds were docked into a crystal structure of JAK2 (Chain A of PDB ID 2B7A¹⁷) using GLIDE v58515 (Schrödinger, LLC) in XP mode using default parameters. During docking, the compound was required to make hydrogen bonds to the backbone of residues Glu-930 and Leu-932. Resulting poses were subsequently filtered through visual inspection. The protein structure was prepared for calculation using the PrepWizard functionality within MAESTRO v9.3.5 (Schrödinger, LLC) retaining chain A and water molecule 139 as the receptor.
- Lucet, I. S.; Fantino, E.; Styles, M.; Bamert, R.; Patel, O.; Broughton, S. E.; Walter, M.; Burns, C. J.; Treutlein, H.; Wilks, A. F.; Rosjohn, J. *Blood* **2006**, *107*, 176.
- (a) Finlay, M. R. V.; Acton, D. G.; Andrews, D. M.; Barker, A. J.; Dennis, M.; Fisher, E.; Graham, M. A.; Green, C. P.; Heaton, D. W.; Karoutchi, G.; Loddick, S. A.; Morgentin, R.; Roberts, A.; Tucker, J. A.; Weir, H. M. *Bioorg. Med. Chem. Lett.* **2008**, *18*, 4442; (b) Barillari, C.; Duncan, A. L.; Westwood, I. M.; Blagg, J.; van Montfort, R. L. M. *Proteins: Struct., Funct., Bioinf.* **2011**, *79*, 2109.
- Van de Waterbeemd, H.; Smith, D. A.; Jones, B. C. *J. Comput. Aided Mol. Des.* **2001**, *15*, 273.
- Compounds **24** and **31** were profiled as racemates.
- Katz, J. D.; Lapointe, B. T.; Dinsmore, C. J. *Org. Chem.* **2009**, *22*, 8866.
- Compounds were dosed by oral gavage to C56bl/6 mice as a solution in 40%PEG400: 50%Trappsol: 10% water. Drug concentrations and pSTAT5 signal were measured at 1, 3, and 8 h.